Determining the Hydrological Representativeness Scale: An Areal Threshold for Detecting Regional Hydroclimatic Signals in Iranian River Basins

Ali Jalalvand

Shahid Chamran University of Ahvaz, Ahvaz, Iran (a.jalalvand@scu.ac.ir)....

ARTICLE INFO

Artlcle history:
Received:
Revised:
Accepted:
Available online:

Keywords:
Regional hydroclimatic influences; Hydrological representativeness scale; Areal threshold; Zonal and azonal basins; Kruskal–Wallis test; Iranian river basins.

TO CITE THIS ARTICLE:

Abstract:
Assessing the impacts of climate change on river discharge requires catchments that reliably reflect regional climatic signals, yet such signals are often masked by local controls, particularly in small and heterogeneous basins. This study determines the minimum basin area—termed the hydrological representativeness scale—above which streamflow primarily reflects regional climate variability rather than local factors. Using 41-year naturalized discharge records from 113 hydrometric stations across five major basins, an iterative Kruskal–Wallis test was applied to specific discharge values to identify the transition from locally dominated to hydroclimatically representative basin behavior. The results identify a transitional zone between 850 and 950 km², with an optimal threshold at approximately 900 km². Above this scale, streamflow becomes more regionally coherent and less variable, whereas smaller basins exhibit stronger local heterogeneity and greater hydrological noise. The robustness of this threshold was confirmed through multiple independent validations, including Dunn's post hoc analysis, inter-station correlation, temporal sub-period testing, runoff coefficient analysis, variability metrics (C_v and C_s/C_v), and sensitivity analysis. Although the numerical threshold is region specific, the proposed methodological framework is transferable to other regions, offering a practical tool for prioritizing representative monitoring basins and supporting water resources planning and related hydroclimatic assessments.

Introduction

Global warming and its associated impacts are no longer just potential threats, but an inevitable reality. When the climate changes, water resources will be among the sectors most affected (Sadoff and Muller 2009). Consequently, this will have far-reaching implications for all aspects of human life. For this reason, water is the first medium through which climate change affects people, ecosystems, and economies. Therefore, water resources management should place its primary focus on climate change adaptation (adaptation meaning using the productive potential of water and limiting its destructive potential). By adapting, humans achieve water security, which enables resilience to future challenges. It should be noted that achieving water security is a systematic process and requires continuous efforts.

Hydroclimatic and hydrological systems are fundamentally coupled, such that a change in one can significantly alter the other (Kingston et al. 2024). Rivers, as critical water sources, are highly vulnerable to these climatic shifts. Research indicates that changing climatic patterns are altering river regimes, affecting flow, water levels, and flooding, which in turn degrades riverine ecosystems and disrupts human systems (Brown et al. 2007; Das et al. 2022). However, monitoring these effects is

complicated because not all basins respond uniformly. Distinct physical characteristics of each watershed—such as geology, soil, and aquifer properties—significantly modulate hydrological events, obscuring the climate-change signal within the system's natural noise. Furthermore, human activities like dam construction add layers of complexity, making the detection of a clear hydroclimatic signal even more challenging.

A key framework for understanding these changes classifies rivers based on the climatic dominance of their flow regimes (Vladimirov 1990; Kovalenko 2007):

1- Zonal rivers exhibit flow regimes that reflect the long-term climatic patterns of their geographical region and remain largely unaffected by local influences.

2- Azonal rivers deviate from the zonal pattern due to the dominant influence of localized factors—such as lakes, wetlands, karst systems, or other geological features.

3- Transregional (or polygonal) rivers have flow regimes influenced by the characteristics of two or more geographical regions, resulting in complex hydrological characteristics.

Therefore, to accurately discern the regional hydroclimatic influences, it is essential to focus on basins that predominantly reflect large-scale climatic signals— i.e., the zonal basins. This approach aligns with established global methodologies for hydrological regionalization and basin classification (e.g., Wilson et al. 2013 for Europe; Gubareva, 2012 for Japan), which are recognized as essential tools for understanding spatio-temporal patterns in river flow regimes and the hydroclimatic processes that drive them.

Figure (1) empirically demonstrates this classification by analyzing global river systems and plotting the relationship between specific discharge (in liters per second per square kilometer) and basin area (in square kilometers).

A foundational premise for this approach is the critical areal threshold: a basin must be sufficiently large to integrate local heterogeneities and manifest regional climate patterns (Kovalenko 1986). Basins exceeding this threshold exhibit a more stable flow-climate relationship, making them reliable indicators for assessing climate impacts on discharge, including extremes (Asabina 2007). This threshold is region-specific, as evidenced by values ranging from 200–1,500 km² in the former Soviet Union to 1,500 km² in parts of Africa (Karasev 1987; Hamidu 2015).

Iran, situated within the global arid and semi-arid belt, has always been highly sensitive to climatic variability. Recent studies indicate that the country is experiencing significant shifts in hydroclimatic patterns and an increasing frequency of extreme events (Jahanshahi et al. 2024), consistent with IPCC (2023) projections. Moreover, these impacts are not spatially uniform; some regions are experiencing decreasing rainfall, while others are experiencing more intense precipitation events (Chaparinia et al. 2025). For instance, studies in the Tehran-Karaj basin project an overall decrease in annual runoff but an increased risk of winter flooding for specific return periods under future climate scenarios (Yousefi Malekshah et al. 2019). Developing a sustainable approach for safeguarding Iran's water resources therefore requires a robust assessment of climate change impacts on rivers, and sound strategic planning depends on it (Ghazi et al., 2025).

Despite the hydrological importance of zonal basins for detecting hydroclimatically influenced changes (climate-driven changes) in river flow, most previous studies have inferred basin-size thresholds using regional statistics or hydroclimatic classifications, without implicitly assuming that discharge recorded at a gauging station adequately represents the integrated hydrological response of the upstream catchment. However, this assumption has rarely been tested empirically. In regions with strong physiographic heterogeneity, a gauging station may reflect only local controls rather than basin-scale climatic signals, leading to misinterpretation of regional hydroclimatic influences on river flow.

Accordingly, this study aims to (i) identify a practical areal threshold for Iranian river basins using a nonparametric statistical approach (the Kruskal–Wallis test), and (ii) quantify the hydrological representativeness scale of gauged catchments based on discharge records from 113 hydrometric

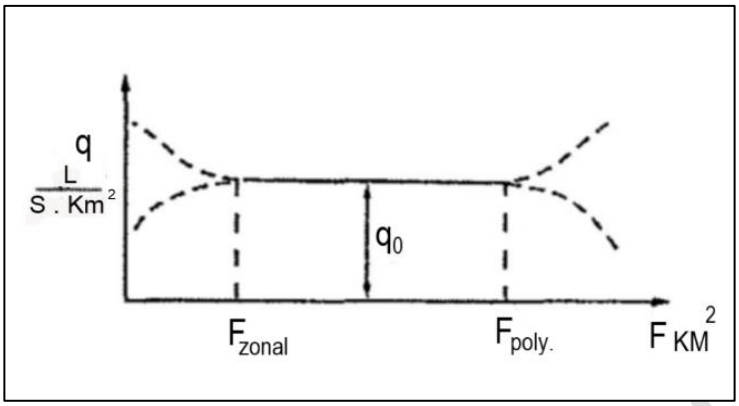


Fig. 1- Changes in specific river discharge relative to river area (Kovalenko 2007).

stations across five major river basins of Iran. The results provide a framework for selecting representative monitoring basins for hydroclimatic impact assessment and support the development of more reliable river monitoring and water management strategies in Iran.

Research Methodology

This study employs a quantitative approach to systematically assess the relationship between watershed area and discharge rates and establish a robust, area-based criterion for distinguishing zonal from azonal watersheds in Iran. The analysis is based on long-term hydrometric data from 113 watersheds that represent the country's diverse hydroclimatic conditions.

Data Quality Control and Naturalization

To ensure the reliability of the hydrological analysis, a rigorous data quality control and naturalization protocol was implemented on the streamflow data from the five studied basins. This involved:

- Selecting a Reference Period with Naturalized Flow: A long-term period (e.g., 1966-2006) preceding major anthropogenic disturbances was chosen as the reference baseline to represent the natural flow regime.
- Testing for and Removing Trends: Stationary and trend-free data series were confirmed using the Mann-Kendall trend test. Any significant trends indicative of gradual anthropogenic impacts, such as land-use change, were statistically removed.
- Accounting for Direct Human Interventions: The impacts of point-source infrastructures (e.g., dams, major diversions) were identified and corrected for by using data from upstream stations or by employing correlation methods with undisturbed reference basins.
- Outlier and Gap Handling: Potentially erroneous data points were identified using graphical methods (e.g., Box-Plots) and cross-referenced with original records. Missing data were infilled using correlation with neighboring stations during the common baseline period to avoid transferring anthropogenic influences.

Through this comprehensive process, we confirm that the final dataset used in this study is homogeneous, trend-free, and representative of the naturalized streamflow potential of the watersheds.

Detection of Threshold Using the Kruskal-Wallis Test

The core of our analytical strategy involved an iterative process of grouping and comparing catchments by area to identify a statistically significant zonality threshold based on specific discharge patterns (to eliminate the effect of drainage area). For this purpose, we selected the Kruskal-Wallis test. This nonparametric method is particularly suitable for our hydrological dataset for three key reasons (Ramachandran and Tsokos 2009):

- It does not require the assumption of normally distributed data.
- It is less sensitive to outliers compared to parametric alternatives.
- It is appropriate for small and unequal sample sizes.

The test was performed using SPSS software (version 16) to assess statistical differences between groups in each iteration.

The implementation procedure was conducted as follows:

First, all 113 catchments were arranged in ascending order by drainage area. For each catchment, mean annual discharge was converted to specific discharge (L s^{-1} km^{-2}) to normalize the effect of basin size. In the initial step, the two smallest catchments were assigned to Group A (the "small-basin" group), while the remaining 111 catchments were assigned to Group B (the "large-basin" group). The Kruskal–Wallis test was then applied to compare specific discharge between the two groups, and the resulting χ^2 statistic and its associated p-value were recorded. In each subsequent iteration, the smallest catchment from Group B was transferred to Group A, thereby gradually increasing the size threshold. The Kruskal–Wallis test was reapplied after each transfer, and the χ^2 and p-values were again recorded. This stepwise procedure was continued until fewer than five catchments remained in Group B.

The overall research workflow, including data preparation, the iterative grouping algorithm, and the statistical testing procedure, is summarized in Figure (2).

To define the zonality threshold, we calculated the Chi-square statistic and its associated p-value for all possible partition points. The optimal threshold was chosen at the point that maximized the Chi-square value, provided that the p-value remained below the 0.05 significance level. With this process, not only can a change point be discerned, but also two hydrological differential regimes can be identified.

Independent Hydrological Validation

To verify that the detected threshold is not merely a statistical artifact, an independent hydrological validation was performed using inter-station discharge correlations. For each pair of hydrometric stations within the same basin, the Pearson correlation coefficient (r) between their discharge time series was calculated. The standard deviation of correlation values (SD(r)) was then computed for groups of catchments with similar drainage areas and plotted against the logarithm of watershed area. This analysis helps clarify the relationship between streamflow behavior and catchment area.

Results and Discussion

A total of 113 catchments with naturalized discharge records, based on 41 years of data, were selected from the Ministry of Energy reports (Ministry of Energy 2009, 2012, and 2013) across five major river basins: the Karun River basin (28 Catchments), Karkheh River Basin (22 Catchments), Sefid Rood River basin (28 Catchments), Aras River basin (19 Catchments), and Hendijan - Jarrahi River basin (16 Catchments). These catchments exhibited a wide range of discharge (0.22 m^3/s in Amugheen in the Aras basin, to 152.16 m^3/s in Tange Pange in the Karun basin) and drainage areas (41 km^2 in Solla, Aras basin to 51,454 km^2 in Gilvan-Ghezel Ozen, Sefid Rood basin) (Appendix A). The discharge data were detrended and naturalized to remove anthropogenic influences such as water withdrawals.

Figure (3) illustrates the distribution of river discharge relative to the upstream area of hydrometric stations, closely resembling Figure (1) and consistent with global patterns. Since the boundary between zonal and azonal river regions is not visually discernible, the nonparametric Kruskal-Wallis test was employed for this analysis.

Figure (4) presents the Chi-square values for all iterations. The peak Chi-square value ($\chi^2 = 5.91$, $p = 0.015$) occurred at iteration 34, indicating the most significant divergence in hydrological behavior between the two groups. The p-value trends across iterations fluctuated between statistical significance and non-significance, as summarized below:

Iterations 1-32: $p > 0.05$ (not significant) - except iteration 3

Iterations 33-41: $p < 0.05$ (significant) – except iteration 39

Iterations 42 - 103: $p > 0.05$ (not significant)

Iterations 104 - 107: $p < 0.05$ (significant)

Iterations 108 - 111: $p > 0.05$ (not significant)

Figure (4) establishes the zonal-azonal boundary in Iran to be between 850 and 950 km^2, with an optimal threshold of 900 km^2 (iteration 34) for assessing hydroclimatic impacts on river regimes. This value is consistent with thresholds reported in other regions, such as 1,500 km^2 in parts of Africa (Hamidu 2015). The 40% discrepancy,

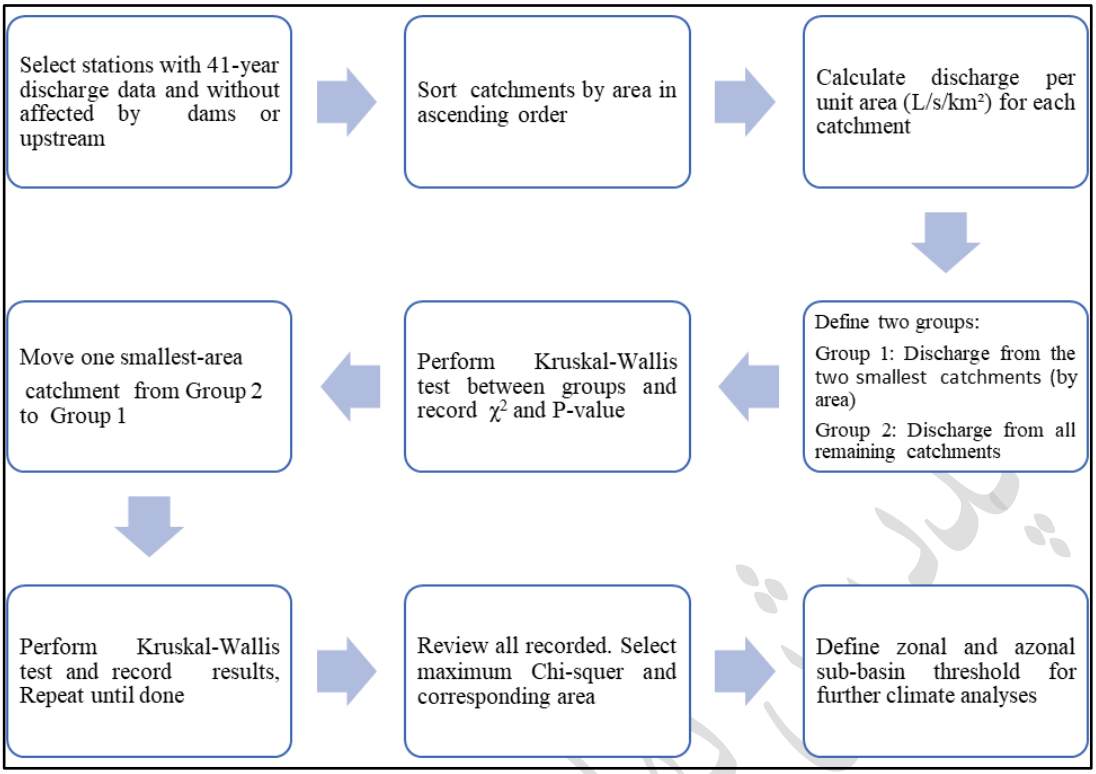


Fig. 2- Workflow Diagram (Iterative nonparametric partitioning algorithm)

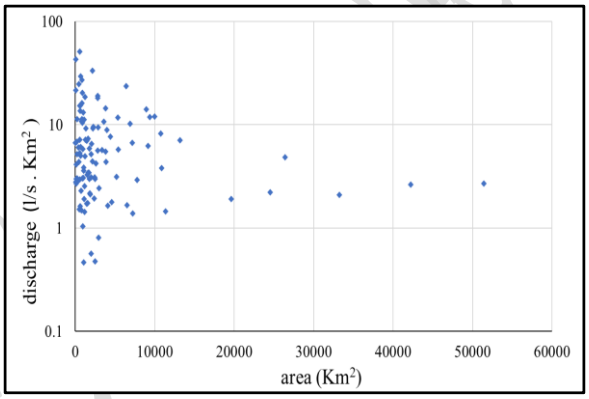


Fig. 3- Showing the distribution of river discharge relative to area

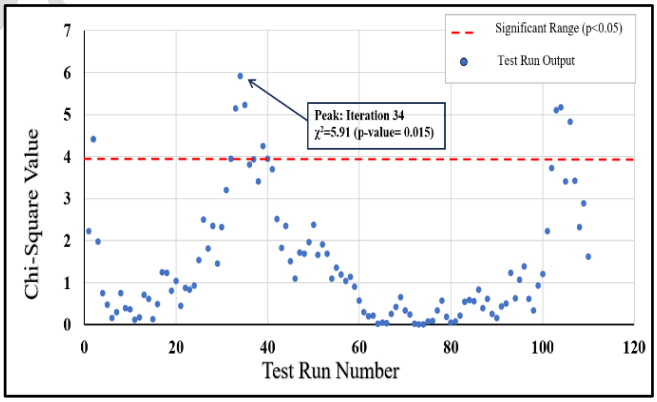


Fig. 4- Trends in Chi-square values across iterations

however, provides important empirical evidence that the spatial scale at which a river basin begins to reflect regional climate- rather than local features- is dictated by the

prevailing hydroclimatic conditions. Consequently, applying a universal areal threshold is invalid, underscoring the need to derive region-specific criteria.

This study's findings contribute to the broader context of hydrological regionalization, a field where diverse approaches address the challenge of identifying homogeneous basins. For instance, methodologies such as those employed by Gubareva (2012) use complex multivariate analyses of a suite of morphometric and physiographic parameters to decipher the causal mechanisms governing runoff generation and to delineate hydrologically homogeneous regions based on structural controls. In contrast, the objective of the present study was not to discover the 'why' of hydrological behavior, but to provide a pragmatic, operational criterion to answer a key management question: 'Beyond what basin area does the hydroclimatic signal prevail over the noise of local factors? The derived area threshold provides water resource managers with a user-friendly tool to prioritize 'zonal' basins—those primarily influenced by climate—as key monitoring sites to assess regional hydroclimatic influences. This approach is founded on the principle that the discharge observed at a hydrometric station is the final product, an integrated manifestation of all controlling factors (both zonal and azonal). By screening basins by areal extent, the influence of azonal factors is minimized, thereby allowing the regional hydroclimatic signal to become dominant and detectable.

The operational value of this threshold is highlighted when considering specific climate change impacts on hydrological extremes. For instance, projections indicating severe reductions in low-flow magnitudes (e.g., Q_{95}) in Iranian catchments (Mozayyan et al. 2013) underscore the importance of identifying basin scales at which hydroclimatic signal can be more clearly distinguished from local variability. The area threshold therefore serves as a practical screening tool for prioritizing larger (zonal) basins within a national climate-impact monitoring network, where regional climatic influences are strongly expressed and hydrologic shifts can be detected earlier and more reliably.

To assess the robustness of the derived area threshold, its validity and sensitivity are examined in the following sections.

Validation and Refinement Using Dunn's Post-Hoc Test

To further validate and statistically refine the distinction between zonal and azonal hydrological regimes identified through the iterative Kruskal–Wallis procedure, Dunn's post-hoc test was systematically applied. As a nonparametric pairwise comparison method, this test is particularly suitable for confirming significant differences between groups following a significant Kruskal–Wallis result. To ensure comprehensive validation, the test was implemented programmatically in R, replicating the core iterative grouping logic across all 110 iterations.

The results from Dunn's test corroborate the primary finding. The most statistically significant divergence in specific discharge between the two groups occurred at Iteration 34 (comparing 35 catchments in Group 1 against 78 in Group 2), corresponding to the areal threshold. At this point, Dunn's test yielded a minimum p-value of 0.0075, confirming a highly significant difference (p-value < 0.01) in hydrological behavior between the groups. This result provides further statistical evidence for the zonal–azonal boundary, as this p-value is more stringent than the initial Kruskal–Wallis p-value of 0.015 obtained at the same iteration.

Scaling Effects on Hydrological Response and Basin Representativeness

To investigate how the hydrological behavior of a sub-basin changes with increasing area, the Pearson discharge correlation coefficient between sub-basins and the downstream reference station was first examined in each basin. The reference station is defined as the largest sub-basin (by area) on the main channel of each of the five basins. This analysis aimed not only to determine the degree of discharge correlation among sub-basins but also to assess the similarity of their hydrographs.

Figure (5) illustrates the relationship between sub-basin discharge correlation and

the reference station as sub-basin area increases. It is clearly evident that discharge correlations in small sub-basins are highly scattered. However, beyond a threshold of approximately 1000 km², all discharge correlation values exceed 0.8.

To further clarify the issue, the relationship between changes in discharge correlation coefficients and basin area was examined by analyzing variations in the standard deviation of the discharge correlation coefficient (SD (r)) as a function of the logarithm of basin area. Figure (6) presents this relationship. Small-scale basins exhibit high SD (r) dispersion, indicating instability in hydrograph response and a strong influence of local factors on basin outflow. As basin area increases, the variability of SD(r) decreases significantly (from 0.07 to 0.023), likely attributable to climatic noise and measurement errors.

The gradual decline in the standard deviation of the correlation coefficient with increasing basin area suggests that, as a basin expands, its drainage network integrates more hydrological units. This integration reduces the influence of localized processes on the overall river response. Consequently, the response becomes increasingly governed by dominant basin-scale controls. Furthermore, the stabilization of SD (r) at the identified areal threshold (~900 km²) suggests that adding more area to the basin does not substantially alter hydrograph behavior. Therefore, discharge measured at the outlet of such basins can be considered representative of the watershed's overall hydrological performance. This scale may be defined as the "hydrological representativeness scale of the basin." These findings can be applied in the selection of hydrometric reference stations, water balance analysis, and calibration of rainfall–runoff models.

Independent Validation Using Pairwise Correlation of Hydrologically Similar Basins

To provide an independent, nonparametric validation of the proposed areal threshold, a complementary analysis was conducted based on pairwise Pearson correlation coefficients between annual specific discharge time series of selected basin pairs.

Seven pairs of basins were selected from the large-size category (>950 km²) and seven pairs from the small-size category (<850 km²). Each pair consisted of two basins within the same parent basin that shared similar climatic and geographic conditions, thereby minimizing the influence of regional climate variability and isolating the effect of basin area on hydrological coherence. The selection was constrained to basins with long-term (41-year) data.

For each pair, the Pearson correlation coefficient (r) was computed using the CORREL function in Microsoft Excel.

The computed correlation coefficients for the seven large-basin pairs were:

>950 km² pairs:

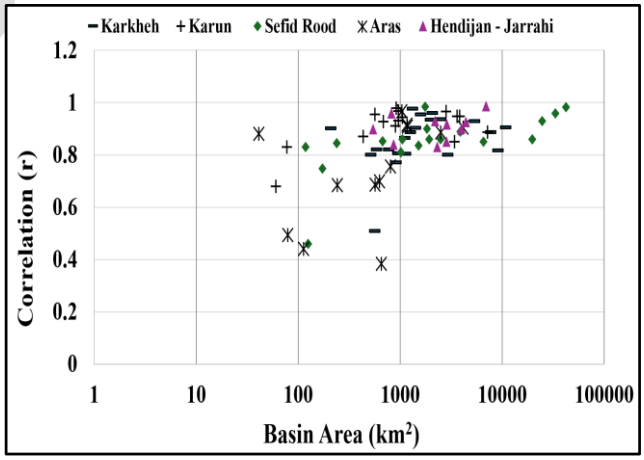


Fig. 5- The relationship between basin area and the correlation coefficient of streamflow between the reference downstream station and the upstream sub-basins.

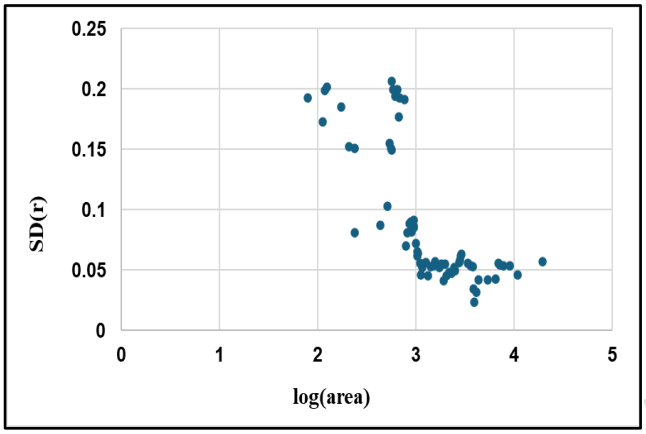


Fig. 6- Variations in the standard deviation of the discharge correlation coefficient (SD(r)) as a function of the logarithm of the basin area.

0.867, 0.854, 0.867, 0.824, 0.819, 0.926, 0.832

(Mean ± SD: 0.855 ± 0.035)

<850 km² pairs:

0.325, 0.718, 0.837, 0.697, 0.590, 0.800, 0.639

(Mean ± SD: 0.658 ± 0.160)

The Pearson correlation coefficients (r) were transformed to Fisher's Z-scores using the standard transformation, because this transformation normalizes the sampling distribution and stabilizes the variance, making the data suitable for parametric comparison.

$$Z=0.5Ln((1+r)/(1-r)) \quad (1)$$

An independent-samples t-test was then conducted to compare the mean Z-scores between the large-basin pairs (n=7) and the small-basin pairs (n=7).

Levene's test confirmed homogeneity of variances ($F = 0.364$, $p = 0.557$). The t-test revealed a statistically significant and substantial difference between the two groups ($t(12) = 3.329$, $p = 0.006$), with a large effect size (Cohen's $d = 1.92$). The mean Z-score for large-basin pairs (1.85 ± 0.62) was markedly higher than that for small-basin pairs (0.45 ± 0.91), indicating significantly greater hydrological coherence among basins exceeding 950 km².

This finding provides independent statistical evidence that basins above the identified areal threshold exhibit synchronized, climate-driven flow regimes, whereas smaller basins remain dominated by local physiographic heterogeneity.

Temporal Validation of the Areal Threshold

To assess the robustness and temporal stability of the identified threshold, the same iterative Kruskal–Wallis procedure was independently applied to two non-overlapping sub-periods: the first 20-year and the second 21-year intervals. The analysis for both sub-periods yielded a nearly identical threshold to that derived from the full 41-year period. Figures (7) and (8) illustrate the results of the iterative Kruskal–Wallis procedure for these two sub-periods. As shown, the highest chi-square value consistently occurred at Iteration 34, reaffirming the characteristic area threshold.

It is noteworthy that a secondary statistically significant peak was observed during the latter stages of the iterative procedure in the analysis of the full dataset Figure (4) as well as in both sub-period analyses (Figures 7 and 8) (e.g., iteration 104 in Figure (4), corresponding to 105 catchments in Group 1 and only 8 in Group 2). However, this peak was deemed spurious and hydrologically insignificant for three principal reasons. First, it represents a highly unbalanced group comparison in which statistical significance may be artificially inflated by an extreme disparity in sample sizes. Second, a threshold that segregates only a minimal number of basins (e.g., eight) lacks practical utility for regional water resources management and planning. Third, the weaker statistical significance (p- value = 0.0115) and the lower associated Z-score

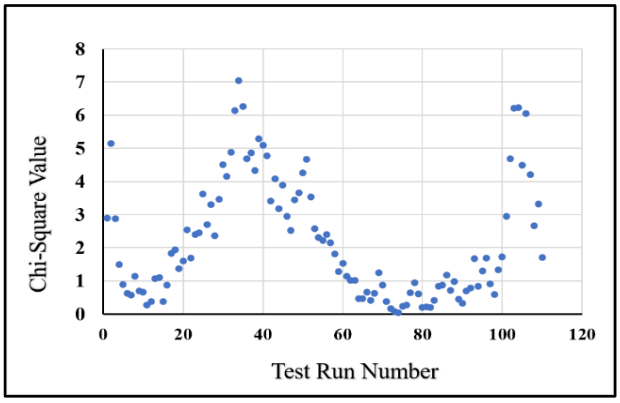


Fig. 7- Trends in Chi-square values across iterations for the first 20-year period

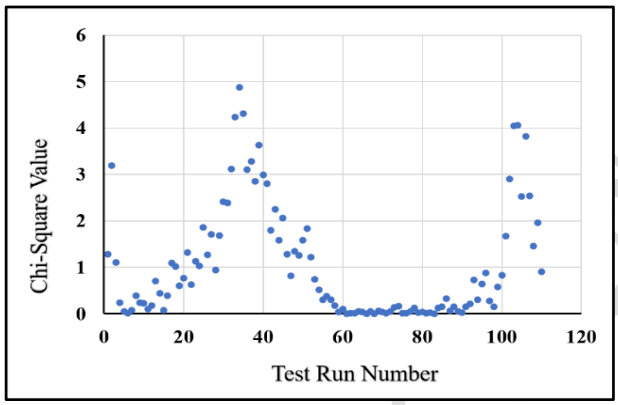


Fig. 8- Trends in Chi-square values across iterations for the second 21-year period

(2.273 vs. 2.431 at Iteration 34) indicate a less robust hydrological differentiation than at the primary threshold. Consequently, this peak was dismissed as a statistical artifact.

Validation Using Runoff Coefficient

To further validate the findings based on specific discharge and to integrally consider the role of precipitation as the primary climatic driver of flow regimes, an additional analysis was conducted using the runoff coefficient. The runoff coefficient, calculated as the ratio of long-term mean naturalized discharge to mean annual precipitation for each basin, serves as an integrated indicator of a basin's efficiency in converting precipitation into surface runoff and reflects the combined influence of climate and watershed characteristics.

The same iterative protocol as in the primary method (the Kruskal-Wallis test) was applied to the runoff coefficient data for the 113 basins (Appendix B). The results of this independent analysis strongly corroborated the study's main finding. The trend of the Chi-square statistic across iterations showed a pattern highly similar to that in Figure (4), with a distinct statistical peak at Iteration 35 (Figure 9). At this peak, the Chi-square statistic was 4.86 with a significance level (p-value) of 0.027, corresponding to basins with an approximate area of 910 km².

The convergence of evidence from specific discharge and runoff coefficient establishes the derived area threshold as a hydroclimatic boundary. This transition marks the shift from local-factor dominance in smaller basins to regional-climate control in larger basins. As such, it offers a practical, scientifically grounded guideline for initial basin screening within a national climate adaptation strategy.

Sensitivity Analysis of Areal Threshold

A comprehensive sensitivity analysis was performed to assess the robustness of the identified areal threshold by examining its response to variations in the grouping methodology. While the primary analysis employed a stepwise approach (transferring one basin at a time), water resource

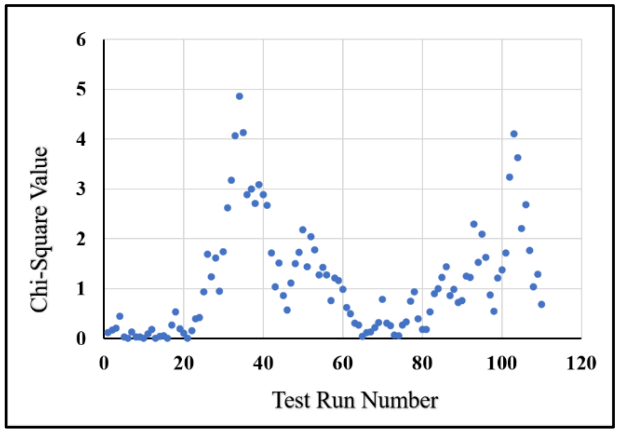


Fig. 9- Trends in Chi-square values across iterations for runoff coefficient

Table 1- Sensitivity of detected areal threshold to grouping step size

Step Size (basins/iteration)	Detected Threshold (km²)	χ^2 Statistic	Deviation from 900 km²	Percentage Deviation
1	910	5.91	10 km²	1.1%
2	914	5.84	14 km²	1.6%
3	914	5.76	14 km²	1.6%
4	896	5.68	4 km²	0.4%
5	950	5.42	50 km²	5.6%
10	1045	4.91	145 km²	16.1%

planning requires evaluating whether the threshold remains stable across different analytical approaches. This analysis therefore addresses a critical practical question: how sensitive is the threshold to the choice of grouping step size within the iterative Kruskal-Wallis procedure?

Six different grouping step sizes were systematically tested (1, 2, 3, 4, 5, and 10 basins per iteration), replicating the core Kruskal-Wallis analytical framework while varying only the rate at which basins were transferred between groups (implemented programmatically in R).

For each step size configuration, the peak χ^2 value and its corresponding areal threshold were identified, and the percentage deviation from the reference area (900 km²) was calculated using equation (2):

$$\text{Deviation (\%)} = (|\text{Threshold}_{step} - 900| / 900) \times 100 \quad (2)$$

Statistical Sensitivity

The sensitivity analysis revealed a remarkably stable threshold across different grouping approaches (Table 1). For the fundamental step size of 1 (basin-by-basin iteration, matching our primary methodology), the detected threshold was 910 km², representing only a 1.1% deviation from the reference area. This minor discrepancy arises from the discrete nature of basin areas—while 900 km² serves as the rounded representative value, the actual statistical optimum falls at 910 km². Four of the six tested configurations showed deviations of less than 5%. The mean deviation across all step sizes was 4.4%, with the χ^2 trends demonstrating consistent peak patterns around the identified optimal threshold (Figure 10).

Visual Validation of Threshold Behavior

In Figure (11), specific discharge is plotted against catchment area on log-log axes, illustrating a scale-dependent transition between azonal (local) and zonal (regional) regimes around the ~900 km² threshold. Figure (12) provides detailed categorization of all 113 basins into three operational groups based on the identified threshold zone. The visualization reveals:

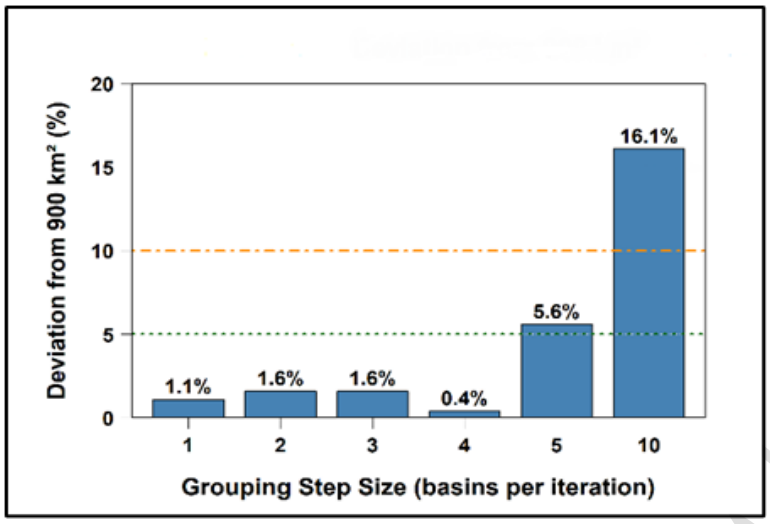


Fig. 10- Sensitivity analysis for stable threshold across different grouping step sizes

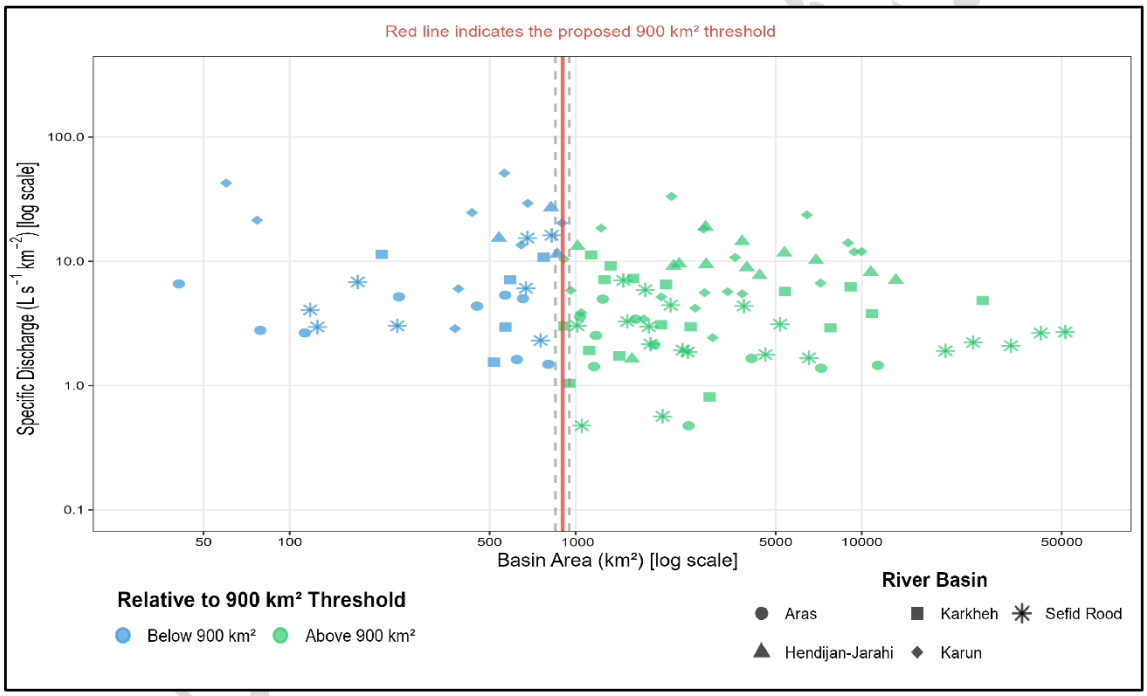


Fig. 11- Hydrological zonation showing separation at 900 km² (red line). Azonal (blue) and zonal (green) regimes exhibit distinct specific discharge patterns on logarithmic axes, visually confirming the statistical threshold

Small basins (<850 km², n=32): Exhibit high specific discharge variability (Figure 12A), consistent with azonal systems where local geological and topographic factors exert primary control.

Transitional basins (850–950 km², n=5): Display intermediate behavior, representing a critical zone where local and regional influences intersect. This group (basins sized 862 to 945 km²) confirms that the threshold is a functional range rather than an abrupt point.

Large basins (>950 km², n=76): Demonstrate relatively uniform behavior with reduced variability, indicative of zonal systems where regional hydroclimatic signals dominate local noise.

The existence of this transitional zone (850–950 km²) explains two key findings from our analysis. First, it clarifies why the statistical procedure identified a range (860–960 km²) rather than a single sharp boundary. Second, it demonstrates why the minor 1.1% difference between the statistical optimum

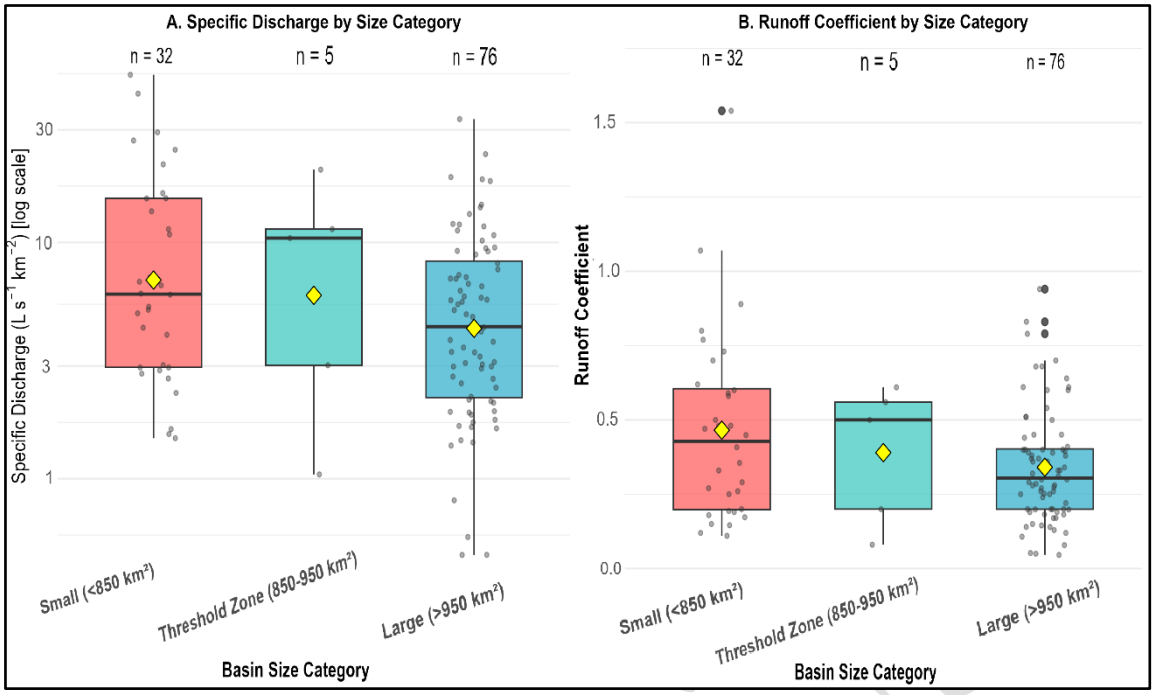


Fig. 12- Comparison of specific discharge and runoff coefficient across basin size zones. (A) Specific discharge variability decreases with increasing basin size, supporting the proposed statistical threshold. (B) Corresponding runoff coefficient patterns show a similar trend. The 850–950 km² transitional zone includes five basins (n = 5) with intermediate behavior between small azonal basins (n = 32; higher variability) and large zonal basins (n = 76; relatively uniform behavior).

(910 km²) and rounded publication value (900 km²) is hydrologically insignificant. Both values reside within the transitional zone where basin behavior exhibits gradual rather than abrupt change.

Scale-dependent variability structure (C_V and C_s/C_V)

Here, the coefficient of variation (C_V) and the C_s/C_V ratio are used as descriptive indicators to examine scale-dependent changes in the magnitude and structure of discharge variability, rather than as variables for formal hypothesis testing.

Figure (13) illustrates clear scale-dependent changes in discharge variability as quantified by the coefficient of variation (C_V). Small catchments (<850 km²) exhibit a wide range of C_V values and pronounced scatter, indicating strong interannual variability in discharge. This behavior reflects the dominance of short flow paths, localized precipitation variability, and limited storage capacity, which together produce highly responsive and irregular runoff regimes.

In contrast, large catchments (>950 km²) display a narrower C_V distribution and reduced variability. The attenuation of discharge variability at larger spatial scales indicates the increasing influence of basin-wide storage, channel routing, and spatial averaging of precipitation inputs. These processes act as low-pass filters that attenuate short-term fluctuations and stabilize streamflow response.

Catchments within the transitional range (850–950 km²) exhibit intermediate C_V values, consistent with a progressive shift from locally controlled streamflow generation to an integrated basin-scale response. The emergence of reduced variability beyond the identified threshold (~900 km²) supports interpreting this threshold as a hydrological integration scale rather than a purely statistical boundary.

Figure (14) illustrates corresponding changes in the C_s/C_V ratio across basin size categories, highlighting scale-dependent shifts in the statistical structure of discharge variability. Small catchments (<850 km²) exhibit a wide dispersion of C_s/C_V values, with frequent extreme values, indicating

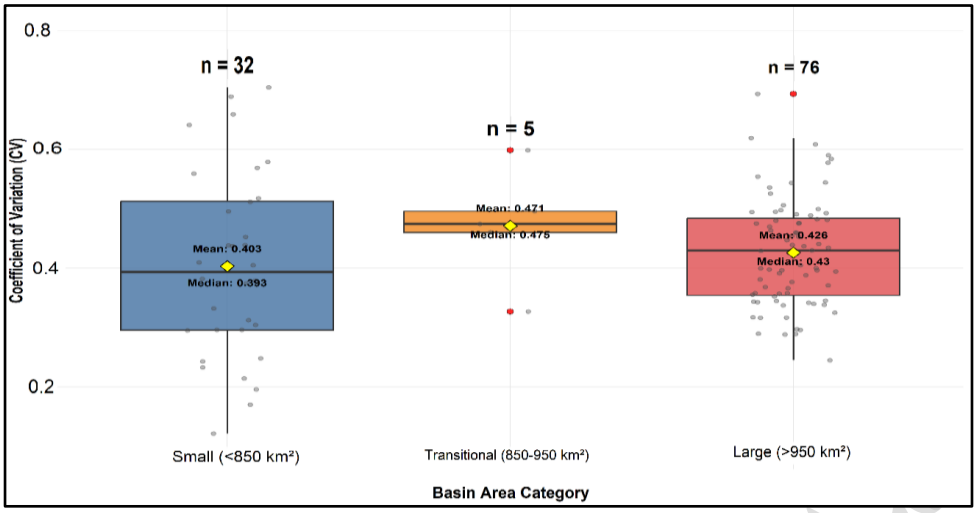


Fig. 13- Variation of the coefficient of variation (C_V) of specific discharge across basin area categories. Boxplots show the distribution of C_V values for small (<850 km^2, n=32), transitional (850–950 km^2, n=5), and large (>950 km^2, n=76) catchments. Individual basins are plotted as circles, with red circles indicating statistical outliers. Horizontal black lines and yellow diamonds represent the median and mean values, respectively

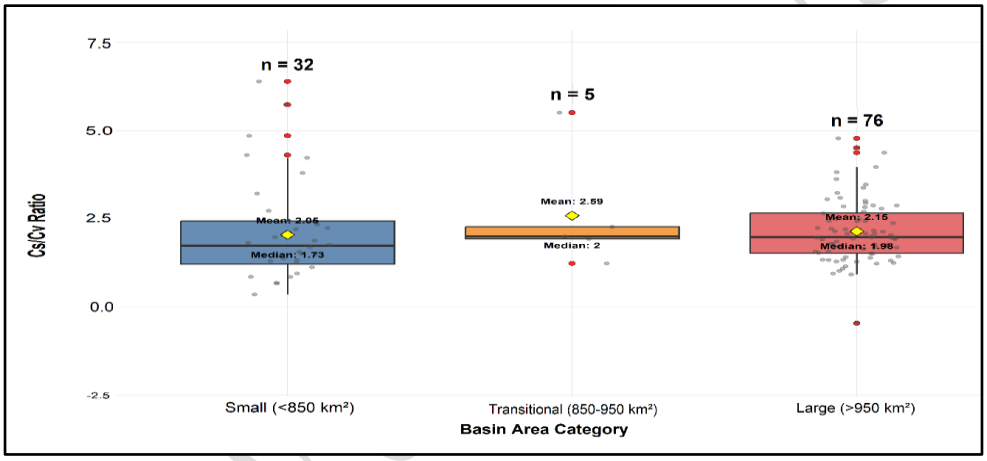


Fig. 14- Comparison of the ratio between the coefficient of skewness (C_s) and coefficient of variation (C_V) across basin area categories. Boxplots summarize C_s/C_V for small (<850km^2, n=32), transitional (850–950 km^2, n=5), and large (>950 km^2, n=76) catchments. Points represent individual basins; yellow diamonds and black horizontal lines denote the mean and median, respectively

irregular, event-driven runoff responses dominated by local controls.

As basin area increases, C_s/C_V values converge toward a quasi-stable range close to 2, particularly in catchments larger than 950 km². This convergence reflects the increasing dominance of the integrated basin response, in which storage and routing processes smooth localized extremes and produce more regular discharge distributions. Catchments in the transitional size range exhibit intermediate Cs/C_V behavior, indicating the coexistence of local-scale variability and basin-scale integration.

Together, the reduced dispersion of C_V and the convergence of C_s/C_V with increasing basin area indicate that the identified threshold (~900 km²) marks a transition in both the magnitude and structure of discharge variability. While C_V characterizes changes in variability intensity, C_s/C_V reflects a change from locally driven, event-scale runoff to integrated, climate-regulated basin behavior. These complementary indicators support the interpretation of the identified threshold as a hydrological integration scale rather than a purely statistical artifact.

Hydrological interpretation of the hydrological representativeness scale (~900 km²)

The statistically derived threshold (~900 km²) likely reflects a hydrologically meaningful integration scale rather than a purely numerical partition. In small catchments, streamflow response is primarily governed by local controls such as lithology, soil permeability, slope configuration, and localized groundwater–surface water interactions. Because these basins are small, spatial precipitation variability and short flow paths produce rapid and irregular runoff responses, leading to high interannual variability in specific discharge. As a result, local geomorphic and hydrogeological characteristics can strongly influence basin behavior.

As catchment area increases, streamflow gradually integrates spatial differences in precipitation and subsurface storage. Larger basins combine the responses of multiple sub-catchments and routing pathways, which increases effective storage and reduces temporal variability in discharge. Channel routing and groundwater contributions act as low-pass filters, damping short-term variability and stabilizing discharge. This spatial averaging effect reduces the influence of localized physiographic controls and enhances the influence of regional hydroclimatic forcing. Consequently, streamflow variability decreases, and discharge becomes more closely related to basin-scale climatic inputs than to local geomorphic conditions.

The transition observed around the identified areal threshold (~900 km²) therefore, defines a hydrological representativeness scale, at which catchment storage and routing processes become sufficiently developed to smooth localized hydrological responses and reveal a coherent hydroclimatic signal. Below this hydrological representativeness scale, runoff generation is dominated by site-specific characteristics, whereas above it, the basin's integrated behavior reflects regional precipitation regimes. This transition thus represents a hydro-geomorphic shift from locally controlled runoff production to climate-controlled flow regulation, providing a physical explanation for the zonal–azonal distinction identified by the hydroclimatic transition analysis.

From an applied perspective, this scale may be useful for hydrological regionalization, model parameter transfer, and interpreting discharge variability in ungauged or sparsely gauged basins.

Interpretative Considerations and Pathways for Future Research

While this statistically derived threshold provides a practical, operational criterion for distinguishing streamflow regimes, its underlying physical drivers require further elucidation. The identified transition zone (~850–950 km²) likely represents the spatial scale at which local hydrogeomorphic heterogeneities (e.g., lithology, soil characteristics, aquifer properties) become integrated, allowing regional hydroclimatic signals to dominate the hydrological response. Future targeted studies in representative basins within this transitional range—equipped with detailed field data—could unravel the specific physiographic controls that modulate the exact location of this areal threshold. Such work would provide a physical basis for the hydroclimatic transition scale presented here, enriching our understanding of scale–climate interactions in semi-arid hydrology.

Conclusions

This study identifies a hydrologically meaningful transition scale that separates locally controlled (azonal) from climate-dominated (zonal) river regimes across major basins in Iran (the hydrological representativeness scale). Analyses of long-term naturalized discharge data consistently indicate that this transition occurs at a basin area of approximately 900 km², beyond which streamflow behavior increasingly reflects regional climatic forcing rather than local variability. The robustness of this threshold is supported by multiple independent validations, confirming that it represents a genuine hydroclimatic integration scale rather than a statistical artifact. Basins exceeding this scale exhibit coherent and representative hydrological responses suitable for climate change impact assessment and regional monitoring, while smaller basins require management

approaches tailored to local-scale controls. Although the numerical value of the threshold is region-specific, the proposed data-driven framework is transferable, provides a practical tool for identifying comparable transition scales in other regions, and can support the screening and prioritization of basins for water resource management and climate change monitoring worldwide.

Conflict of Interest

The authors declared no potential conflicts of interest concerning the research, authorship, and publication of this article. Confirmation.

Funding

The authors received no financial support for the research, authorship, and publication of this article.

Data Availability Statements

Data Availability Statement: All information and results are presented in the text of the article.

Authors' contribution

Author: Ali Jalalvand: Conceptualization, Methodology, Formal analysis, Data curation, Investigation, Software (for statistical analyses), Validation, Visualization, Writing – Original Draft, Writing – Review & Editing.

Acknowledgment

This research has no acknowledgments.

References

1- Asabina, E., 2007. Multilevel River classification as the methodological basis for analysis of maximum runoff values in different geographical regions, *The International Association of Hydrological Sciences (IAHS*), pp. 365–373.

2- Brown, L. E., Hannah, D. M. and Milner, A. M., 2007. Vulnerability of alpine stream biodiversity to shrinking glaciers and snowpacks. *Global Change Biol*. 13(5), pp. 958–966. https://doi.org/10.1111/j.1365-2486.2007.01341.x

3- Chaparinia, F., Hadei, M., Yaghmaeian, K., Hadi, M. and Naddafi, K., 2025. Evaluation of climate indices related to water resources in Iran over the past 3 decades. *Sci Rep* 15, 11846. https://doi.org/10.1038/s41598-025-95370-7

4- Das B. K., Bayen S., Prasad, S. and Sarkar, U. K., 2022. Impact of Climate Change on River Ganga: recent status and mitigation. *Science and Culture*. 88 (11-12). pp. *397-399.* https://doi.org/10.36094/sc.v88.2022.Impact_of_Climate_Change_on_River_Ganga.Das.397.

5- Ghazi B., Salehi H., Cheshami M., Zeydalinejad N. and Thuy Linh, N. T., 2025. Projection of climate change impact on main climate variables and assessment of the future of Köppen–Geiger climate classification in Iran. *Acta Geophysica*. 73, pp. 2017–2027. https://doi.org/10.1007/s11600-024-01457-6.

6- Gubareva, T. S., 2012. Classification of river basins and hydrological regionalization (as exemplified by Japan). *Geography and Natural Resources*, 33, pp. 74-82. https://doi.org/10.1134/S187537281201012X.

7- Hamidu, D., 2015. *Long-term assessment of probability distributions of multi-year evaporation from African territory under climate change*. Dissertation, Russian State Hydrometeorological University, Saint Petersburg, Russia. (In Russian)

8- Intergovernmental Panel on Climate Change (IPCC), 2023. Climate Change 2021- The Physical Science Basis: Working Group I *Contribution to the Sixth Assessment Report of the Intergovernmental Panel on Climate Change.* Cambridge University Press, Cambridge. https://doi.org/10.1017/9781009157896.

9- Jahanshahi, A., Booij, M. J., Patil, S. D. and Gupta, H., 2024. An ensemble-based projection of future hydro-climatic extremes in Iran. *Journal of Hydrology*, 642, 131892. https://doi.org/10.1016/j.jhydrol.2024.131892.

10- Karasev, I. F., 1987. 'Optimal density and principles of placing a network of hydrological observation stations', in *the dynamics of riverbed flows. Collection of scientific papers* (Interuniversity). Leningrad: Leningrad State University. (In Russian)

11- Kingston, D.G., Ionita, M., Stahl, K. and Van Dijk, A., 2024. Chapter 2 – Hydroclimatology. In: Tallaksen, L.M. and van Lanen, H.A.J. (Eds.), Hydrological Drought: Processes and Estimation Methods for Streamflow and Groundwater, *Second Edition. Amsterdam: Elsevier*, pp. 21–47. https://doi.org/10.1016/B978-0-12-819082-1.00012-6

12- Kovalenko, V. V., 1986. *Hydrometric Assessment of River Flow with Elements of Stochastic Approach*. Study guide. Russian State Hydrometeorological University, Saint Petersburg. (In Russian)

13- Kovalenko, V.V., 2007. *Partially Infinite Hydrology*. Russian State Hydrometeorological University, Saint Petersburg. (In Russian)

14- Ministry of Energy, 2009. *Studies for updating Iran National Water Master Plan in the Hendijan-Jarrahi river basin*. Volume 3: Surface Water and Sediment. Fars Parab Engineering Company. (In Persian)

15- Ministry of Energy, 2012. *Studies for updating Iran National Water Master Plan in the border basins of western Karkheh, Karun, Jarrahi and Zohreh. Volume 4: surface water resources (quantitative and qualitative), up to 2006*. Bahan Sad Consulting Company. (In Persian)

16- Ministry of Energy, 2012. *Studies for updating the Iran National Water Master Plan in the basins of Aras, Urmia, Talesh-Anzali Wetland, Sefid Rood, Sefid Rood-Haraz, Haraz-Qarasu, Gorgan Rood, and Atrak. Volume 4: Report on surface water resources (quantitative and qualitative) of Sefid Rood basin*. Mahab Ghods Consulting Company. (In Persian)

17- Ministry of Energy, 2013. *Water balance: 13 study areas located in the Aras River Basin. Report on the second volume of hydrology*. Lar Consulting Engineering Company. (In Persian)

18- Ministry of Energy, 2013. *Water balance: 13 study areas located in the Aras River Basin. Report on the second volume of hydrology*. Lar Consulting Engineering Company. (In Persian)

19- Mozayyan, M., Akhoond Ali, A. M., Massah Bavani, A. R., Radmanesh, F. and Zohrabi, N., 2013. The Impact of Climate Change on Low Flows (Case Study: Sepid Dasht Sezar). *Journal of Agricultural Sciences and Irrigation Engineering*, 38(2), pp. 1-19. (In Persian)

20- Ramachandran, K. M. and Tsokos, C. P., 2009. Mathematical Statistics with Applications. *Academic Press.* Boston.

21- Sadoff, C. and Muller, M., 2009. *Water management, water security and climate change adaptation: early impacts and essential responses*. TEC Background Papers No. 14. Stockholm: Global Water Partnership (GWP) Technical Committee (TEC).

22- Vladimirov, A. M., 1990. *Hydrological computations*. State Hydrological Institute. Leningrad. (In Russian)

23- Wilson, D., Hannah, D. M. and McGregor, G. R., 2013. A large-scale hydro climatological perspective on western European river flow regimes. *Hydrology Research.* 44 (5), pp. 809-833. https://doi.org/10.2166/nh.2012.201.

24- Yousefi Malekshah, M., Ghazavi, R. and Sadatinejad, S., 2019. Evaluating the Effect of Climate Change on Runoff and Maximum Flood Discharge in the Dry Area (Case Study: Tehran-Karaj Basin). *ECOPERSIA* 7(4), pp. 211-221.

Appendix A -The discharge characteristics of the utilized rivers

row	station name	discharge (m^3/s)	area (Km^2)	row	station name	discharge (m^3/s)	area (Km^2)
			Karun basin				
1	Betari	18.22	896	15	Tange Zardalo	4.04	1045
2	Patave	50.98	2800	16	Zarin Derakht	1.09	379
3	Keta	38.76	3609	17	Armand	119.63	9986
4	Barez	126.12	8953	18	Dozdak Abad	28.87	563
5	Kohe Sokhte	7.31	3010	19	Behesht Abad	20.91	3820
6	Vanai	2.56	60	20	Darkash	9.49	910
7	Rahim Abad	5.95	1729	21	Gilyan	10.71	434
8	Dorud	19.36	3400	22	Sepid Dasht	47.95	7174
9	Maroak	5.6	960	23	Sepid Dasht 2	19.91	680
10	Kamendan	1.65	77	24	Tange Pange Sezar	112.1	9410
11	Solegan	10.3	1992	25	Tange Pange	152.2	6432
12	Pole Kareh Bast	15.81	2821	26	Dashte Bozorg	10.98	2616
13	Morgak	71.96	2162	27	Jelogir	8.74	645
14	Lordegan	2.34	389	28	Zoor Abad	22.72	1227
			Sefid Rood basin				
29	Bianloo	16.15	5181	43	Telvar Dehkalan	0.72	238
30	Telvar	10.93	6538	44	Mianeh	9.52	2146
31	Gamishkan	3.94	1825	45	Chipni	10.3	1468
32	Garegoni	37.37	19618	46	Telvar-Hssan Khan	4.6	2465
33	Inki Kand	4.57	2365	47	Mianeh- Grango	16.91	3870
34	Palti	1.18	173	48	Mah Neshan	54.46	24511
35	Sarcham	8.18	4604	49	Onlig	0.48	118
36	Pole Dokhtar	69.68	33235	50	Nesar-e Olya	10.34	1751
37	Motor Khaneh	5.38	1802	51	Shadi Abad	1.14	2013
38	Kohsar	3.08	1012	52	Pole Delbaran	0.5	1050
39	Stor	111.77	42240	53	Chatab	4.07	670
40	Gilvan	139.18	51454	54	Gham Chogha	1.74	754
41	Gling	13.33	824	55	Firoz Abad	4.98	1515
42	Baghklaye	10.43	678	56	Mehtar	0.37	125
			Hendijan – Jarrahi basin				
57	Jarrahi -Moshrake	87.84	10754	65	Dehemolla	92.63	13163
58	Kopal- 3	2.57	1574	66	Pole Flor	33.83	4396
59	Jokanak	21.89	2300	67	Khir Abad	27	2857
60	Mashin	9.82	862	68	Naz Makan	13.39	1015
61	Cham Nezam	62.77	5365	69	Gachsaran	70.47	6918
62	Tang-e Takab	55.18	3818	70	Tange Berim	22.14	820
63	Iding	53.78	2844	71	Batoon	35.26	3966
64	Grab	8.28	539	72	Kohsangan	20.12	2196
			Aras River basin				
73	Samian	6.81	4119	83	Merakand Gator Chai	9.96	7210
74	Solla	0.27	41	84	Mazraeh	3.28	654
75	Amugheen	0.22	79	85	Mashiran	16.55	11379
76	Gorale Olya	6.18	1244	86	Mozafar Abad	1.18	2482
77	Ghale Jogh	3.72	1036	87	Mahlazan	1.65	1159
78	Kasin	1.25	241	88	Musa Gholi	1.01	623
79	Klibar	1.97	452	89	Hir	0.3	113
80	Koze Toporagi	1.19	802	90	Pamchi Ardabil	3.03	567
81	Gilandeh	2.98	1177	91	Mako	5.55	1620
82	Merakand Agh Chai	4	1880				

Appendix A continued

row	station name	discharge (m^3/s)	area (Km^2)	row	station name	discharge (m^3/s)	area (Km^2)
			Karkheh River Basin				
92	Aran (Gharb)	6.14	1988	103	Khosro Abad (Shahab)	0.99	950
93	Aghajanbalaghi	0.8	518	104	Dar toot	7.52	2522
94	Baraftab	2.14	1115	105	Do Ab (Ghamasiyab)	22.72	7770
95	Pole Chehreh	41.25	10860	106	Do Ab (Inarak)	8.98	1260
96	Pole Dokhtar (Kashkan)	57.06	9140	107	Sarabe Seyed Ali	8.36	773
97	Tanghe Sazin	128.02	26436	108	Firozabad (Firozan)	2.76	914
98	Tanghe Siyab	1.68	568	109	Gorbaghestan	30.85	5391
99	Cham-e Anjir	11.58	1590	110	Kaka Reza	12.72	1132
100	Hojat Abad	12.2	1325	111	Noor Abad (Gharb)	4.2	590
101	Hydar Abad (Dinavar)	13.51	2070	112	Vargach	2.39	210
102	Khers Abad	2.46	1420	113	Vasaj	2.38	2940

پذیرش نهایی - قبل از چاپ

Appendix B- Runoff coefficient of the utilized catchments

row	station name	Runoff coefficient	area (Km^2)	row	station name	Runoff coefficient	area (Km^2)
			Karun basin				
1	Betari	0.61	896	15	Tange Zardalo	0.28	1045
2	Patave	0.68	2800	16	Zarin Derakht	0.15	379
3	Keta	0.7	3609	17	Armand	0.64	9986
4	Barez	0.6	8953	18	Dozdak Abad	1.54	563
5	Kohe Sokhte	0.19	3010	19	Behesht Abad	0.36	3820
6	Vanai	0.194	60	20	Darkash	0.56	910
7	Rahim Abad	0.14	1729	21	Gilyan	0.89	434
8	Dorud	0.32	3400	22	Sepid Dasht	0.2	7174
9	Maroak	0.37	960	23	Sepid Dasht 2	0.8	680
10	Kamendan	0.173	77	24	Tange Pange Sezar	0.38	9410
11	Solegan	0.29	1992	25	Tange Pange	0.79	6432
12	Pole Kareh Bast	0.38	2821	26	Dashte Bozorg	0.3	2616
13	Morgak	0.94	2162	27	Jelogir	0.62	645
14	Lordegan	0.26	389	28	Zoor Abad	0.83	1227
			Sefid Rood basin				
29	Bianloo	0.33	5181	43	Telvar Dehkalan	0.33	238
30	Telvar	0.17	6538	44	Mianeh	0.33	2146
31	Gamishkan	0.26	1825	45	Chipni	0.61	1468
32	Garegoni	0.19	19618	46	Telvar-Hssan Khan	0.26	2465
33	Inki Kand	0.28	2365	47	Mianeh- Grango	0.399	3870
34	Palti	0.48	173	48	Mah Neshan	0.199	24511
35	Sarcham	0.22	4604	49	Onlig	0.58	118
36	Pole Dokhtar	0.2	33235	50	Nesar-e Olya	0.61	1751
37	Motor Khaneh	0.3	1802	51	Shadi Abad	0.079	2013
38	Kohsar	0.27	1012	52	Pole Delbaran	0.052	1050
39	Stor	0.25	42240	53	Chatab	0.355	670
40	Gilvan	0.25	51454	54	Gham Chogha	0.2	754
41	Gling	0.77	824	55	Firoz Abad	0.252	1515
42	Baghklaye	0.73	678	56	Mehtar	0.449	125
			Hendijan – Jarrahi basin				
57	Jarrahi -Moshrake	0.395	10754	65	Dehemolla	0.34	13163
58	Kopal- 3	0.182	1574	66	Pole Flor	0.37	4396
59	Jokanak	0.4	2300	67	Khir Abad	0.4	2857
60	Mashin	0.5	862	68	Naz Makan	0.44	1015
61	Cham Nezam	0.51	5365	69	Gachsaran	0.45	6918
62	Tang-e Takab	0.54	3818	70	Tange Berim	1.07	820
63	Iding	0.68	2844	71	Batoon	0.39	3966
64	Grab	0.6	539	72	Kohsangan	0.41	2196
			Aras River basin				
73	Samian	0.15	4119	83	Merakand Gator Chai	0.145	7210
74	Solla	0.7	41	84	Mazraeh	0.59	654
75	Amugheen	0.29	79	85	Mashiran	0.14	11379
76	Gorale Olya	0.51	1244	86	Mozafar Abad	0.046	2482
77	Ghale Jogh	0.285	1036	87	Mahlazan	0.107	1159
78	Kasin	0.47	241	88	Musa Gholi	0.19	623
79	Klibar	0.408	452	89	Hir	0.25	113
80	Koze Toporagi	0.146	802	90	Pamchi Ardabil	0.5	567
81	Gilandeh	0.199	1177	91	Mako	0.274	1620
82	Merakand Agh Chai	0.182	1880				

Appendix B continued

row	station name	Runoff coefficient	area (Km^2)	row	station name	Runoff coefficient	area (Km^2)
			Karkheh River Basin				
92	Aran (Gharb)	0.2	1988	103	Khosro Abad (Shahab)	0.08	950
93	Aghajanbalaghi	0.11	518	104	Dar toot	0.17	2522
94	Baraftab	0.12	1115	105	Do Ab (Ghamasiyab)	0.2	7770
95	Pole Chehreh	0.24	10860	106	Do Ab (Inarak)	0.4	1260
96	Pole Dokhtar (Kashkan)	0.34	9140	107	Sarabe Seyed Ali	0.48	773
97	Tanghe Sazin	0.31	26436	108	Firozabad (Firozan)	0.2	914
98	Tanghe Siyab	0.18	568	109	Gorbaghestan	0.36	5391
99	Cham-e Anjir	0.39	1590	110	Kaka Reza	0.6	1132
100	Hojat Abad	0.5	1325	111	Noor Abad (Gharb)	0.27	590
101	Hydar Abad (Dinavar)	0.45	2070	112	Vargach	0.12	210
102	Khers Abad	0.13	1420	113	Vasaj	0.05	2940

پذیرش نهایی - قبل از چاپ